

# Jets in multiparticle production in and beyond geometry of proton-proton collisions at the LHC

M.Yu. Azarkin, I.M. Dremin, M. Strikman

June 17, 2014

## Abstract

Experimental findings by CMS on properties of jets and underlying events at high multiplicities in proton-proton interactions at 7 TeV are interpreted as an indication of increasing role of central collisions with small impact parameters. The value of the average impact parameter of the pp collisions as a function of the soft hadron multiplicity is estimated. We find an indication that the rates of different hard processes observed by CMS and ALICE universally depend on the underlying event charged-particle multiplicity until it becomes four times higher than average. It is shown that the increase of the overlap area of colliding protons is not sufficient to explain the rate of jet production in events with charged-particle multiplicity that is more than three times higher than average. New mechanisms are necessary, like interaction of protons in rare configurations of higher than average gluon density. Such mechanisms are not included in the present Monte Carlo event generators. Further studies are proposed.

## 1 Introduction

Multi-particle production in proton-proton (pp) collisions is governed by several mechanisms of hadron dynamics. The geometry of the collision plays a crucial role in the relative contributions of these mechanisms. Both non-perturbative and perturbative QCD mechanisms contribute to the hadron production.

At the parton level, each event of the inelastic particle production is treated as a combination of hard and soft parton-parton interactions plus partonic remnants of colliding protons. The hard parton-parton interactions result in jets, which appear in final state as well-collimated bunches of hadrons. At large enough transverse momenta of jets, they can be treated within perturbative QCD. The softer components, including also soft ingredients of jets, combine in the so-called underlying event (UE). The interplay between soft and hard contributions certainly depends on the collision energy and on the impact parameter of the collision. The complicated structure of the interaction region was discussed in many papers and, in particular, in [1, 2].

Several important features of inelastic pp interactions emerge from the analysis of the data on elastic pp scattering (using  $s$ -channel unitarity) and analysis of the transverse parton spread as extracted from hard *exclusive* processes like  $\gamma + p \rightarrow J/\psi + p$ . First, one finds that

in interactions at the LHC energies protons are completely absorptive at small central area and have a large semi-transparent peripheral zone (Sec. 2.1). Second, one finds that partons with large fractions of proton energy ( $x$  above  $10^{-3}$ ) are concentrated in the central absorptive area. A detailed and up-to-date review of the two-scale picture of proton is given in [2].

The goal of the paper is to derive information about dependence of hadron production on the impact parameter using the observables, exploiting the fact that the relative importance of hard and soft interactions strongly depends on the impact parameter. We use the most recent experimental studies of processes with a hard trigger and high multiplicities. We determine up to which maximum charged-particle multiplicities, the impact parameter picture works and where other mechanisms start to dominate. An important tool in our studies is the ratio of the multiplicity of the hard subprocesses for a given range of multiplicity to the one in bulk of inelastic events. We demonstrate that this ratio exhibits *universality pattern* when plotted against  $N_{\text{ch}}/\langle N_{\text{ch}} \rangle$ . This result is practically the same for jet production with  $p_{\text{T}} > 5$  GeV/ $c$  and  $p_{\text{T}} > 30$  GeV/ $c$ , as studied by CMS for associated charged particles detected in  $|\eta| < 2.4$  range. Moreover, the universality holds when we compare the CMS ratios with those reported by ALICE for  $J/\psi$ , D, B-meson production [3] in a factor of 3 smaller  $|\eta|$  interval. We also argue that a new regime sets in at  $N_{\text{ch}}/\langle N_{\text{ch}} \rangle \geq 3$ , corresponding to very central collisions in which the rate of the hard-probe multiplicity exceeds the maximum value allowed by the geometry of the collision. This new regime may correspond to selection of configurations in the colliding nucleons with larger than average relatively-small- $x$  ( $x \sim 10^{-3} - 10^{-2}$ ) gluon density.

The paper is organized as follows. In Sec. 2 we review the transverse geometry of bulk and hard-probe triggered pp collisions. Next, in section 3, we analyse some recent LHC results [4–7] as well as more detailed data of CMS collaboration [8] on properties of jets and UE in different charged-particle multiplicity intervals. In section 4, we use jet production as a way to test (calibrate) centrality dependence of events on their multiplicity. We present our conclusions and suggest strategies for further studies in Sec. 5.

## 2 Geometry of soft and hard pp collisions

### 2.1 Proton structure obtained from elastic scattering

The impact of the proton structure on inelastic processes can be viewed from the overlap function defined by the unitarity condition for elastic scattering amplitudes. It has been directly computed [9] from experimental data obtained by the TOTEM collaboration [10, 11] for pp scattering at 7 TeV. The corresponding formula in the impact parameter representation is

$$G(s, b) = 2\text{Re}\Gamma(s, b) - |\Gamma(s, b)|^2, \quad (1)$$

where  $G(s, b)$  is the overlap function determining the inelastic profile of colliding protons, and

$$i\Gamma(s, b) = \frac{1}{\sqrt{\pi}} \int_0^\infty dq q f(s, t) J_0(qb). \quad (2)$$

is the Fourier-Bessel transform of the elastic scattering amplitude  $f(s, t)$  related to the differential cross section as

$$\frac{d\sigma}{dt} = |f(s, t)|^2. \quad (3)$$

and normalized as

$$\sigma_{tot}(s) = \sqrt{16\pi} \text{Im}f(s, 0). \quad (4)$$

The smallness of the real part of  $f(s, t)$  corresponding to small  $\text{Im}\Gamma(s, b)$  implies that one can compute  $G$  with high precision either directly from experimental results (see Fig. 3 in [9]) or assuming the Gaussian profile of the elastic contribution  $\Gamma(s, b)$  (see Fig. 4 in [2]). The obtained shapes of  $G(s, b)$  (see Fig. 1 (a)) are similar and show the pattern with rather flat shoulder at small impact parameters  $b$  with subsequent quite steep fall-off. Attempts to fit it by a Gaussian fail because the plateau up to  $b \approx 0.4 - 0.5$  fm is very flat. This is discussed in more details in [12].

When compared to ISR results [9], the overlap function and, consequently, the blackness (opacity) of protons at 7 TeV somewhat increases in the central region approaching complete saturation. At the same time, a much stronger increase, about 40 %, is observed in the peripheral region near 1 fm. Therefore, the periphery starts to play an increasing role in multiparticle production.

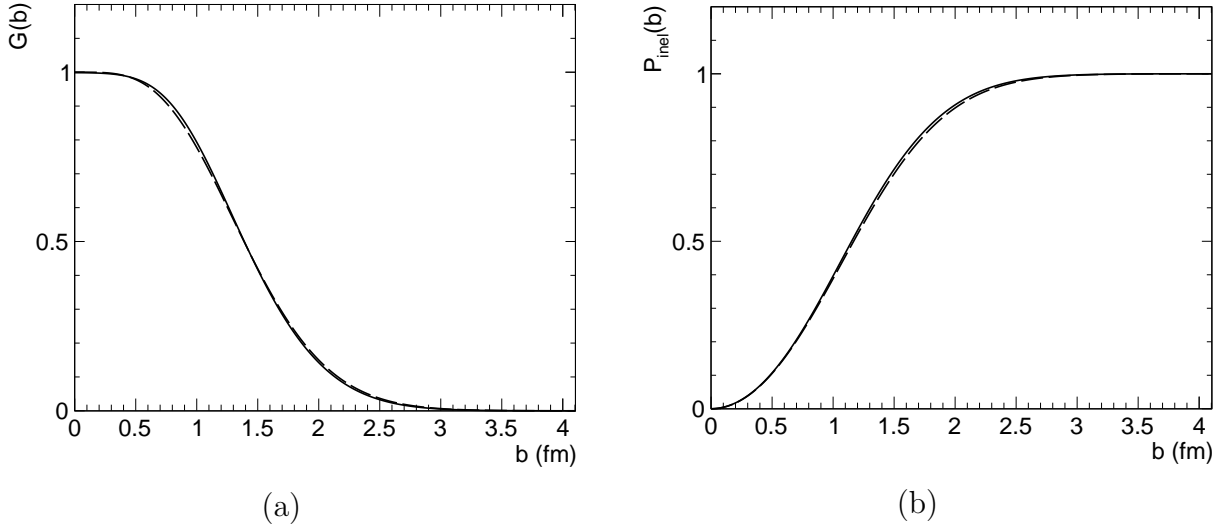


Figure 1: Overlap function (a) and probability of inelastic collision with an impact parameter smaller than  $b$  (b), according to [9] (solid lines) and [2] (dashed lines).

To illustrate the interplay between the black and gray regions we compute the relative contribution of the impact parameters smaller than  $b$  to the inelastic cross section:

$$P_{inel}(b) = \int_0^b d^2b G(s, b) / \sigma_{inel}(s), \quad (5)$$

where  $\sigma_{inel}$  - inelastic cross section of pp collisions. One can see from Fig. 1 (b) that the main contribution to the inelastic cross section originates from the gray area while the dark region ( $b \leq 0.4$  fm) constitutes only about 8 %.

## 2.2 Geometry of dijet production

The transverse distribution of partons in nucleons is given by the generalized parton distributions  $f_j(x, Q^2, t)$ , which are measured in exclusive hard processes. In these processes we

consider  $Q \sim p_T^{\text{jet}}$ . Their Fourier transform,  $f_j(x, Q^2, \rho)$ , determines the geometry of the inclusive hard interactions [13]. The probability that the dijet collision occurs at a given  $b$  is

$$P_2(x_1, x_2, b|Q^2) \equiv \int d^2\rho_1 \int d^2\rho_2 \delta^{(2)}(\mathbf{b} - \rho_1 + \rho_2) \times F_g(x_1, \rho_1|Q^2) F_g(x_2, \rho_2|Q^2), \quad (6)$$

where  $\rho_{1,2} \equiv |\rho_{1,2}|$  are the transverse distances of the two partons from the center of their parent protons [13] and the relation  $f_j(x, Q^2, \rho) = f_j(x, Q^2)F_j(x, \rho|Q^2)$  holds. One finds that the transverse spread of  $F_g(x, \rho|Q^2)$  slowly increases with decrease of  $x$  at fixed  $Q^2$  and slowly decreases with increase of  $Q^2$  for fixed  $x$ .

The distributions of probabilities of hard and soft interactions are compared in Fig.4 in [2]. One can see that  $b$  distribution for hard processes is much more narrow than for bulk events. This is reflected in the probability of small  $b$  for hard collisions (see plot of  $\int_0^b d^2b P_2(b)$  in Fig. 2) to be much higher than for the bulk inelastic collisions (Fig. 1b).

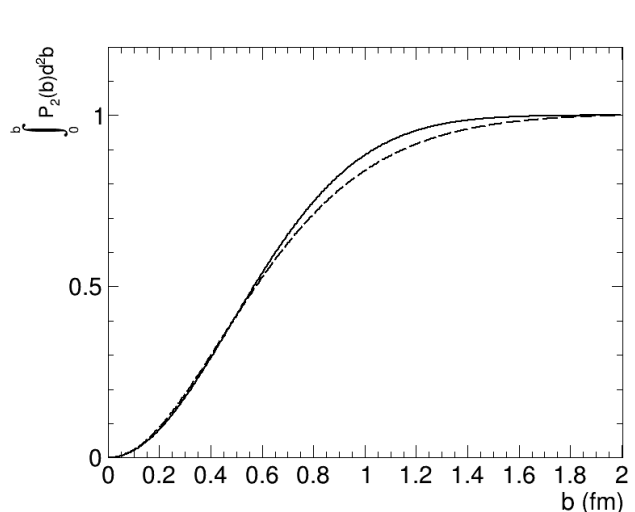


Figure 2: Fraction of the inclusive jet cross section originating from impact parameters from 0 to  $b$ . Solid and dashed lines represent two parameterizations of  $P_2(b)$  as given by Eq. (11) in [2].

### 3 Jet and UE

In this section, we show the connection between standard UE studies and recent study of jet properties as a function  $N_{\text{ch}}$ , exploiting only variables used in these studies, and propose the way to its interpretation. In Sec. 4, we will elaborate on the interpretation and substantiate it with more experimental data.

The UE properties are usually studied with reference to the direction of the particle or of the jet with largest  $p_T$ . Both approaches have advantages and disadvantages. The leading jet is more directly related to the initial parton, however it can be affected by UE contribution. While the leading charged particle is less related with the parent parton, it is not affected by UE. Usually, three distinct topological regions in the hadronic final state are thus defined by

the azimuthal angle difference  $\Delta\phi$  in the plane transverse to the beam between the directions of the leading object (particle or jet) and other hadrons. Hadron production in the near-side region with  $|\Delta\phi| < 60^\circ$  and in the away-side region with  $|\Delta\phi| > 120^\circ$  is expected to be dominated by the hard parton-parton scattering and radiation. Thus, UE structure can be best studied in the transverse region with  $60^\circ < |\Delta\phi| < 120^\circ$ .

A number of recent experimental UE studies use the above described techniques [4–7]. ALICE and ATLAS collaborations use a leading charged particle as a reference, while CMS collaboration uses a leading charged-particle jet. Despite very different pseudorapidity ranges of ALICE and ATLAS experiments ( $\eta < 0.8$  and  $\eta < 2.5$ ), their results are very close. Of particular interest is particle density in transverse region defined as follows:

$$\mu_{\text{tr}} = \frac{N_{\text{ch}}^{\text{tr}}}{\Delta\eta\Delta(\Delta\phi)}, \quad (7)$$

where  $N_{\text{ch}}^{\text{tr}}$  is the charged-particle multiplicity in the transverse region,  $\Delta\eta$  is the pseudorapidity range studied,  $\Delta(\Delta\phi)$  is the azimuthal width of the transverse region. The transverse charged-particle density as a function of leading object at  $\sqrt{S} = 7$  TeV is shown in Fig. 3. The dependence saturates at some  $p_{\text{T}} = p_{\text{T}}^{\text{crit}}$ , which is  $\approx 4 - 5$  GeV/ $c$  and  $\approx 8$  GeV/ $c$  for leading charged particle and leading charged-particle jet techniques, respectively. According to the two-scale picture of the proton structure described in Sec. 1 and elaborated in Ref. [2], the observed plateau corresponds directly to the plateau in Fig. 1(a) at  $b \leq 1.0$  fm because larger  $p_{\text{T}}^{\text{leader}}$  implies smaller  $b$  than in minimal bias events and can be interpreted as an indication of the dominance of the central collisions.

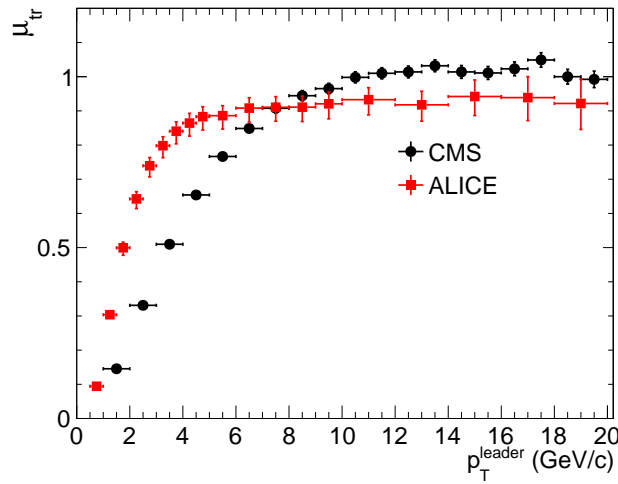


Figure 3: Charged-particle density in the transverse region as a function of  $p_{\text{T}}$  of leading object (CMS - charged-particle jet, ALICE - charged particle). CMS analyses particles with  $p_{\text{T}} > 0.5$  GeV/ $c$  and  $|\eta| < 2.4$ , ALICE -  $p_{\text{T}} > 0.5$  GeV/ $c$  and  $|\eta| < 0.8$ .

Since we aim to reveal a connection between UE studies [4–7] and studies of jet properties as function of  $N_{\text{ch}}$  [8], we need to estimate the  $N_{\text{ch}}$  that corresponds to the plateau of transverse multiplicity density. The  $N_{\text{ch}}$  in [8] is defined as a total number of charged particles with  $\eta < 2.4$  and  $p_{\text{T}} > 0.25$  GeV/ $c$ , while  $\mu_{\text{tr}}$  is obtained with charged particles with

$p_T > 0.5 \text{ GeV}/c$ . From Fig. 3 we can see that the transverse multiplicity density saturates at  $\mu_{\text{tr}}^{\text{sat}} \approx 1.0$ . The charged-particle multiplicity of UE can be roughly estimated in assumption of flat  $\eta$ -distribution as follows:

$$N_{\text{ch}}^{\text{UE}} = \mu_{\text{tr}}^{\text{sat}} \delta\eta \delta\phi \approx 30, \quad (8)$$

where  $\delta\eta = 4.8$ ,  $\delta\phi = 2\pi$  are the pseudorapidity and azimuthal angle ranges used in [8]. Moreover, one should account for different  $p_T$  cuts of charged particles. The correspondence of UE charged-particle multiplicities for different  $p_T$  thresholds is obtained using PYTHIA 6 z2\* simulation, which describes UE properties quite well:

$$N_{\text{ch}}^{\text{UE}}(p_T > 0.25 \text{ GeV}/c) = 1.9 \cdot N_{\text{ch}}^{\text{UE}}(p_T > 0.5 \text{ GeV}/c). \quad (9)$$

Eq. (9) gives approximately 60 charged particles with  $p_T > 0.25 \text{ GeV}/c$ , belonging to the UE when it reaches a plateau. To obtain the total charged-particle multiplicity of an event, one should account a jet contribution. According to tables 4 and 5 of [8], a jet contains 5 particles on average, and the jet rate for  $50 < N_{\text{ch}} \leq 80$  is  $\approx 1$  jet per event. The second, recoiled jet is usually wider and consists of softer particles, and thus may be not found by a jet finding algorithm. This is clearly seen in Fig. 2 of Ref. [4]. Therefore, we conclude that at least 10 charged particles come from jets, and the total  $N_{\text{ch}}$ , where collisions become central, equals  $\approx 70$ .

Results on jet production as a function of  $N_{\text{ch}}$  presented in [8] substantiate the analysis of the previous paragraph. Indeed, we see from table 4 of Ref. [8], that average  $p_T$  of jets with threshold of  $p_T > 5 \text{ GeV}/c$  lies between 7–8  $\text{GeV}/c$ . This value matches to the  $p_T^{\text{crit}}$  at which central pp collisions may occur (see Fig. 3). Therefore, the jet rate at the thresholds 5  $\text{GeV}/c$  can serve as a measure of collision centrality. From that table, one can see that events starting from  $N_{\text{ch}} \approx 60$ –70 have one jet. This means that the most central collision geometry is reached around these values of  $N_{\text{ch}}$ . Other mechanisms should be responsible for  $N_{\text{ch}}$  higher than 70, rather than increasing overlapping area of colliding protons. Indeed, present MC event generators completely fail to describe the charged-particle jet rate with  $p_T$  thresholds of 30  $\text{GeV}/c$  for  $N_{\text{ch}} > 70$  (Fig. 7 of [8]). We conclude, that the estimate of  $N_{\text{ch}}$  of central events obtained from UE studies is consistent with the value obtained from the jet studies as a function of  $N_{\text{ch}}$ .

## 4 The impact parameter dependence and beyond

In Sec. 2.2, we have demonstrated that the probability of the central collisions is rather small. It is instructive to compare it with the probability to have multiplicity larger than given  $N_{\text{ch}}$ , shown in Fig. 4. From the comparison of this plot with the plot for the probability distribution of inelastic events over  $b$  (see Fig. 1(b)), one can make the correspondence between average impact parameter and  $N_{\text{ch}}$  (Fig. 5). We see, that events with  $N_{\text{ch}}(p_T > 0.5 \text{ GeV}/c, |\eta| < 2.4) \geq 35$  mostly originate from collisions with  $b \leq 0.4 \text{ fm}$ . Their probability is about 5 %. However, measured values of  $N_{\text{ch}}$  reach  $\approx 100$ . Such high values (3 times higher than for  $b = 0.4 \text{ fm}$ ) can not be produced even in absolutely head-on collision, if one relies merely on geometric arguments, since possible increase of overlapping area does not exceed ten-percent level.

It was shown in Ref. [15], that ratio of the inclusive rate of hard signals at fixed  $b$  to the average one in bulk events is given as follows:

$$R(b) = P_2(b) \sigma_{\text{inel}}. \quad (10)$$

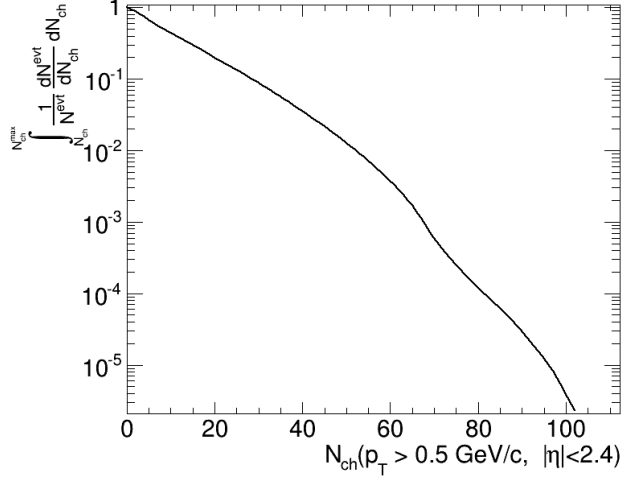


Figure 4: Fraction of events with  $N_{\text{ch}} > N_{\text{ch}}^{\text{fixed}}$ . The  $N_{\text{ch}}$  is defined as a number of stable charged particles with  $p_{\text{T}} > 0.5 \text{ GeV}/c$  and  $|\eta| < 2.4$ . The  $N_{\text{ch}}$  distribution is taken from [14].

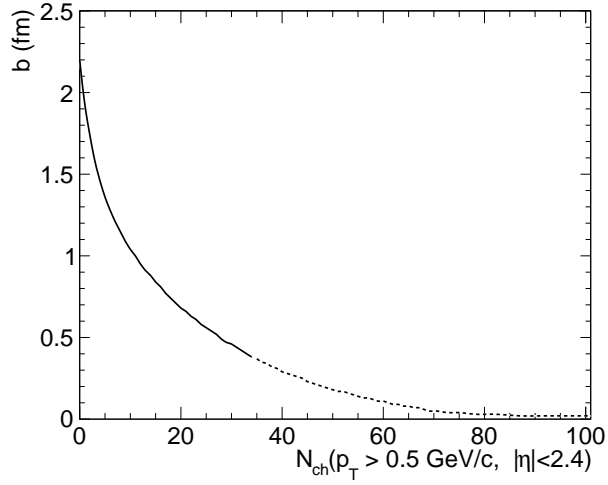


Figure 5: Correspondence between impact parameter and  $N_{\text{ch}}$ .  $N_{\text{ch}}$  is defined here as a number of charged particles with  $|\eta| < 2.4$  and  $p_{\text{T}} > 0.5 \text{ GeV}/c$ . Since events with  $N_{\text{ch}} > 35$  are effectively central as shown below, the correspondence is not valid there.

We take the inelastic cross-section to include events for which any traces of collision are observed in the detector (such events are further called minimum bias). In particular, we refer to the CMS experiment, using their phase space. Therefore, inelastic cross-section taken from [16]  $\sigma_{inel} = 55$  mb should be used for further relevant computations. Thus, a change of the impact parameter of the collision explains values of the ratio (Eq. 10) up to  $R \sim 3.8 - 4.2$  (Fig. 6). It is worth noticing that  $R$  flattens out already for  $b \leq 0.3 \div 0.4$  fm.

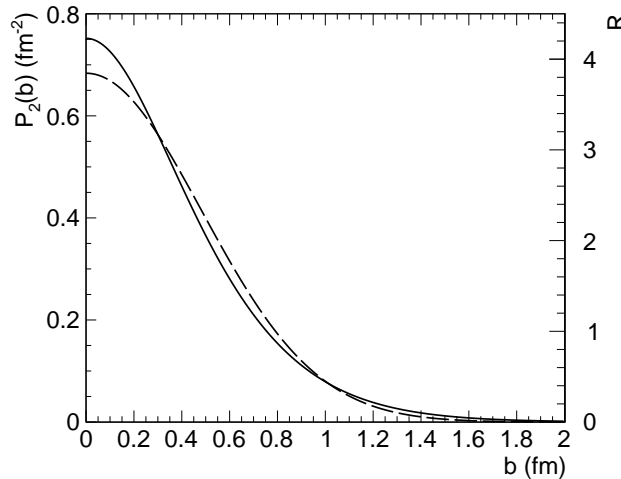


Figure 6: Geometric probability for two gluons to collide (left y-axis) and inclusive jet production rate with respect to the bulk one (right y-axis). Solid and dashed lines represent two parameterizations of  $P_2(b)$  as given by Eq. (11) in [2].

We have extracted  $R$  for charged-particle jets for two  $p_T$  thresholds,  $p_T^{\text{ch,jet}} > 5$  GeV/ $c$  and  $p_T^{\text{ch,jet}} > 30$  GeV/ $c$ , from the data taken from Ref. [8] and presented them in Figs. 7(a, b). The ratios show a very strong increase beyond  $N_{\text{ch}} \sim 80$ . To compare Eq. (10) with the data in Figs. 7 (a, b) we need ideally to plot the rate of jet production as function of  $N_{\text{ch}}^{\text{UE}}$ . Experimentally, the purest way to measure the rate is to select jets produced in one bin of rapidity with multiplicity measured in another bin of rapidity. By doing this, we would avoid the contribution of the hadrons produced in the hard trigger component of the event. In practice, with the current data, we can only try to correct roughly for this effect by using MC simulations (PYTHIA 6 z2\*) to estimate the average charged-particle multiplicity in the selected jets:  $\Delta N_{\text{ch}} = 10$  (15) for  $p_T^{\text{ch,jet}} > 5$  (30) GeV/ $c$ . Hence, to correct for the jet contribution we need to reduce the experimental ratios by a factor  $P(N_{\text{ch}})/P(N_{\text{ch}}^{\text{UE}})$  and plot them as a functions of the  $N_{\text{ch}}^{\text{UE}}$ , which is  $N_{\text{ch}} - \Delta N_{\text{ch}}$  here. The differential  $N_{\text{ch}}$  distribution used for computation of the corrections is taken from [14]. Since the low- $N_{\text{ch}}$  events have large fluctuations in  $|\eta|$ , the correction is not reliable for  $N_{\text{ch}} \leq 50$  and the corresponding points are not plotted in Figs. 7(a, b). One can see that the corrected ratios are approximately the same for two  $p_T$  cuts. This is consistent with the hypothesis that the rates are determined by the initial state of colliding protons.

It is worth noticing, that ALICE has performed studies of a similar quantity,  $R$ , i.e. the ratio of the  $J/\psi$  multiplicity as a function of  $N_{\text{ch}}$  normalized to minimum bias  $J/\psi$  multiplicity [3]. They also reported the same ratio for  $D$  and  $B$ -meson production. The observed dependences of  $R$  on  $N_{\text{ch}}/\langle N \rangle$  are very similar to the one we observe after correcting for the jet contribution



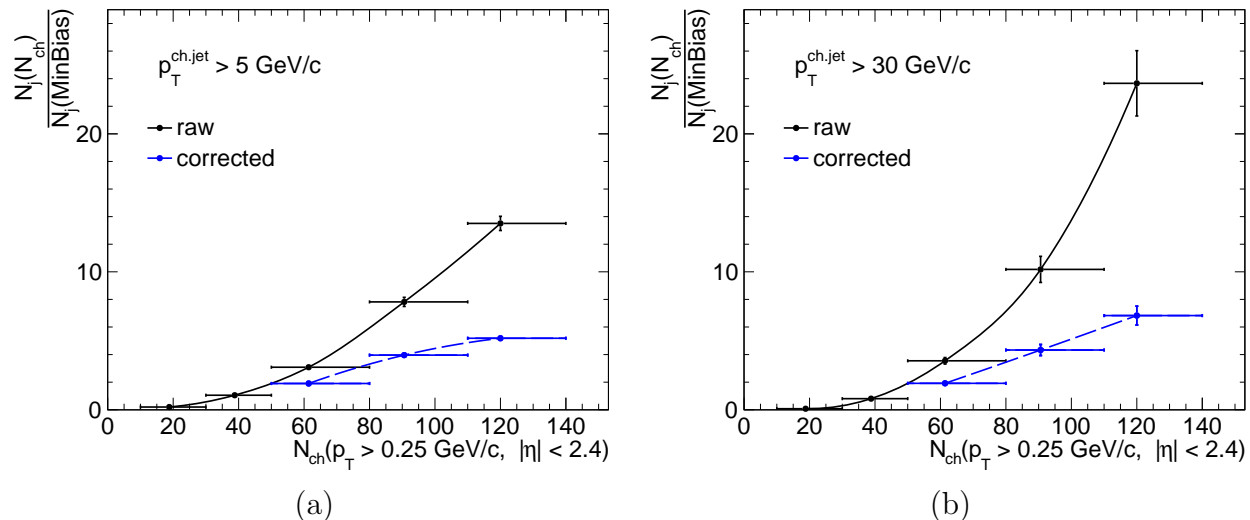


Figure 7: Ratio of  $N_j$  at given  $N_{ch}$  to  $N_j$  of bulk events: (a) - for charged-particle jet  $p_T^{\text{ch,jet}} > 5 \text{ GeV}/c$ , (a) - for charged-particle jet  $p_T^{\text{ch,jet}} > 30 \text{ GeV}/c$ . The black solid lines represent data sorted according to total  $N_{ch}$ . Dashed blue lines represent the ratio if the data would be sorted according to  $N_{ch}^{\text{UE}}$  (note, that the data points are plotted using total  $N_{ch}$ ). To correct the total  $N_{ch}$  to the  $N_{ch}^{\text{UE}}$ , one needs to subtract  $\approx 10$  ( $15$ ) particles for  $p_T^{\text{ch,jet}}$  threshold of  $5$  ( $30$ )  $\text{GeV}/c$ .

(Fig. 8). It is worth emphasizing here, that similarity between  $R$  in the two measurements is highly non-trivial as the rapidity intervals used for determination of  $N_{ch}$  differ by a factor of  $\sim 3$ .

We mentioned above that the inclusive rate of the jet production at given  $b$  as compared to the bulk rate can be calculated using the information about spatial (transverse) gluon distributions in nucleons (Eq. (11) of [2]). Hence, it is provocative to consider relative contributions of different bins in  $N_{ch}$  to the total inclusive rate of jet production. The results are presented in Fig. 9 (a,b) for  $p_T^{\text{ch,jet}} > 5 \text{ GeV}/c$  ( $30 \text{ GeV}/c$ ). Since the median of the  $P_2$  distribution corresponds to  $b \sim 0.6 \text{ fm}$ , we conclude that  $N_{ch} \sim 60$  should roughly correspond to that median value of impact parameter. Also, the corrected value of the ratio,  $R$ , for third domain, which corresponds to average  $b$  of dijet collisions, has a value of about 2 that is consistent with the expectations of Eq. (10) for average  $b$ .

Moreover, the highest multiplicity points for both  $p_T^{\text{ch,jet}}$  cuts correspond to  $R$  well above 4.0 indicating that new mechanisms play a dominant role in this case. The rate of jet production in the collision with a trigger is proportional to the  $g_1 \cdot g_2/S$ , where  $g_1$  and  $g_2$  are the gluon densities in the configurations of nucleons dominating for a particular trigger and  $S$  is the effective area of overlap, cf. Eq. 6. Hence, one possibility [15] is that the rare high- $N_{ch}$  events are produced in collisions of protons in configuration with gluon fields, that are significantly stronger than average gluon density [15]:

$$\frac{(g_1 g_2 / S)_{N_{ch} / \langle N_{ch} \rangle \sim 4 \div 5}}{\langle g_1 g_2 / S \rangle} \sim 2 \quad (11)$$

Probability of such large fluctuations of the gluon field in one or both nucleons is very small – on the scale of  $10^{-2}$ , see discussion in [15]. Hence, this scenario explains the much smaller

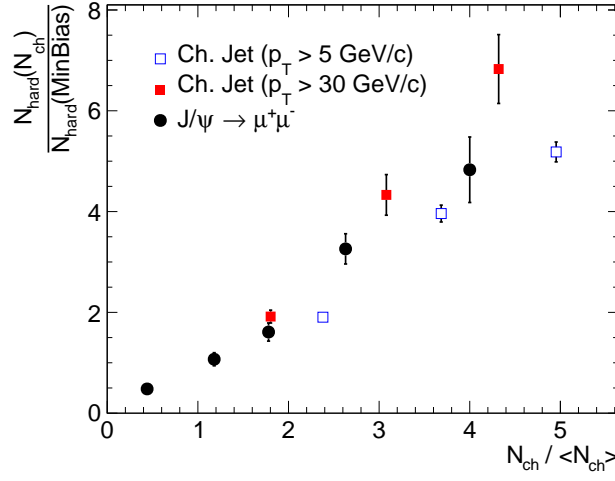


Figure 8: Relative yield of hard momentum processes as a function of  $N_{ch}$ , which does not include particles originating from the hard interactions.

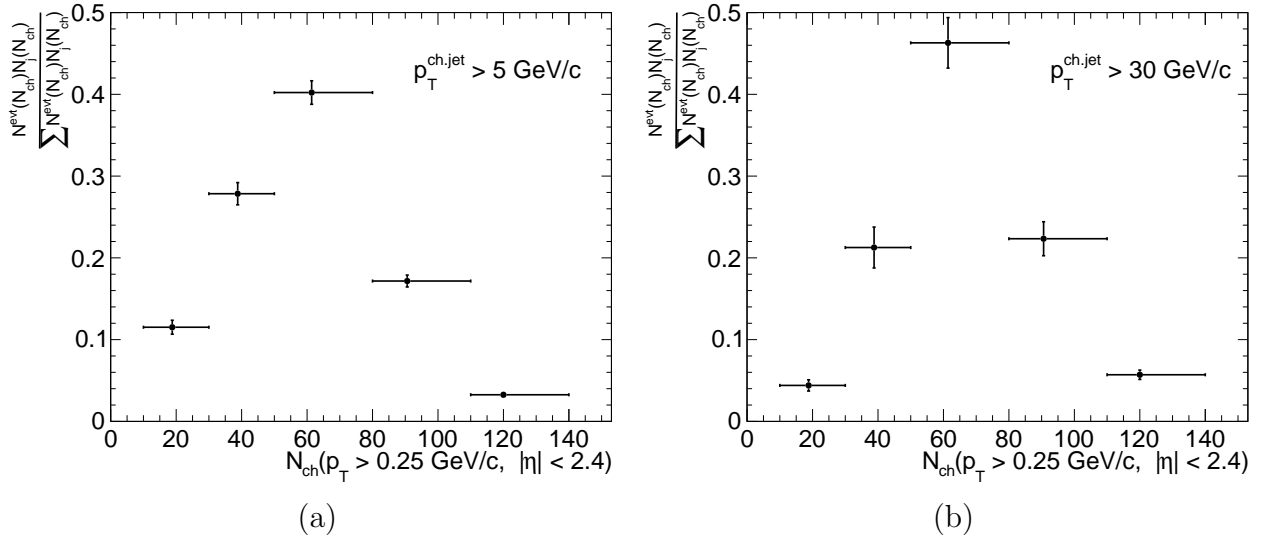


Figure 9: Inclusive jet production as a function of  $N_{ch}$ : (a) - for charged-particle jet  $p_T^{\text{ch,jet}} > 5$  GeV/c, (b) - for charged-particle jet  $p_T^{\text{ch,jet}} > 30$  GeV/c.

probability of these events than the one given by the geometry of the collisions as well as the similar value of the enhancement for events with different jet transverse  $p_T^{\text{ch,jet}}$ . Another source could be contribution of the higher-order QCD processes, that are not properly accounted or not accounted at all in event generator models. However, it is not likely that they would generate the same enhancement for very different  $p_T^{\text{ch,jet}}$  cuts.

Note also, that the measured charged-particle multiplicity reaches values of 170-180 [14]. Then, determining the rate of jet production for these collisions may open a window on the properties of very rare configurations in nucleons.

## 5 Summary and conclusions

The role of proton geometry in multiparticle production at LHC energy has been studied using various experimental data. With the help of hard probes we obtain information about the inner regions of the protons. At LHC energies, the core of protons became absolutely absorptive due to high parton density. Collisions, involving the cores, usually result in high-multiplicity events. Such events contain a large number of high- $p_T$  jets. We have used the dependence of the jet multiplicity on the charged-particle multiplicity studied in [8] as a tool to look inside proton interaction region. We compute the ratio,  $R$ , of the jet multiplicity in the charged-particle multiplicity intervals (corrected for the hard contribution) to one in minimum bias events. The value of the ratio is determined by the geometry of the pp collision up to  $N_{\text{ch}} / \langle N_{\text{ch}} \rangle \sim 3.0$ , corresponding to the average impact parameters of 0.4 fm. We have argued that at higher multiplicities one enters a regime of increase of  $R$ , which is not described by geometry of pp collisions. Our analysis of the LHC data strongly suggests that for  $N_{\text{ch}} > 70$  (at 7 TeV), for which the process is dominated by rare central collisions, where colliding protons fluctuate into special high-density gluon configurations. This suggests that the events in which ridge was observed prominently also originate from similar collisions. Also, we find an indication that the rates of different hard processes observed by CMS and ALICE universally depend on  $N_{\text{ch}}$  until it becomes three times higher than average, where geometry effects dominate. This is consistent with the hypothesis that these rates are predominantly determined by the initial state of colliding protons. Moreover, we observe that it holds even for higher values of  $N_{\text{ch}} / \langle N_{\text{ch}} \rangle$  (up to 4) for  $x$  in the  $10^{-2} \div 10^{-3}$  interval. Hence, it would be highly desirable to extend these observations for a wider  $x$ -range and also to study jet production for larger  $N_{\text{ch}}$  to see whether the jet rate continues to grow, and whether this growth is different for small and moderate  $x$  ( $x > 0.05$ ). Fluctuations of the gluon density may increase relative importance of the multiparton interaction (MPI) mechanism of jet production. Thus it would be worthwhile to try to determine the rate of MPI in the high multiplicity events.

More detailed studies are also highly desirable. In particular, it would be preferable to study dependence on the multiplicity of the underlying event rather than on the total multiplicity. It would be also interesting to study events where multiplicity is significantly smaller than average. One may expect that these events originate from large  $b$  collisions, where the interaction is dominated by the exchange of a single Pomeron. Since properties of the Pomeron do not depend on  $b$ , in this scenario  $R$  should be practically independent on  $\langle N_{\text{ch}} \rangle$ .

Another possible direction for experimental studies would be to investigate how the production of leading baryons (for example, production of leading neutrons with  $x_F \geq 0.3$ ) is correlated with  $N_{\text{ch}} / \langle N_{\text{ch}} \rangle$ . Indeed, it was argued [17] that the neutron yield in the proton fragmentation region drops with an increase of the centrality of the  $pp$  collisions and also de-

creases faster with increase of  $x_F$ . If so, one expects that, with increase of  $N_{\text{ch}}/\langle N_{\text{ch}} \rangle$ , the neutron multiplicity for large  $x_F \geq 0.3$  will diminish and it will be very strongly suppressed for  $N_{\text{ch}}/\langle N_{\text{ch}} \rangle \geq 4$ .

## 6 Acknowledgments

M. Azarkin and I. Dremin are grateful for support by the RFBR grants 12-02-91504-CERN-a, 14-02-00099, and the RAS-CERN program. M. Strikman's research was supported by DOE grant No. DE-FG02-93ER40771. we thank T. Rogers for valuable comments. M. Strikman thanks Leonid Frankfurt for numerous discussions and also would like to thank CERN for hospitality, where this work started.

## References

- [1] T. Sjöstrand and M. van Zijl, “Multiple parton-parton interactions in an impact parameter picture”, *Phys. Lett. B* **188** (1987) 149.
- [2] L. Frankfurt, M. Strikman, and C. Weiss, “Transverse nucleon structure and diagnostics of hard parton-parton processes at LHC”, *Phys. Rev. D* **83** (2011) 054012.
- [3] ALICE Collaboration, “Open-charm production as a function of charged particle multiplicity in pp collisions at  $\sqrt{s} = 7$  TeV with ALICE”, (2013). [arXiv:1309.6570](#).
- [4] CMS Collaboration, “First Measurement of the Underlying Event Activity at the LHC with  $\sqrt{s} = 0.9$  TeV ”, *Eur. Phys. J. C* **70** (2010) 555, [arXiv:1006.2083](#).
- [5] CMS Collaboration, “Measurement of the Underlying Event Activity at the LHC with  $\sqrt{s} = 7$  TeV and Comparison with  $\sqrt{s} = 0.9$  TeV ”, *JHEP* **9** (2011) 109, [arXiv:1107.0330](#).
- [6] ATLAS Collaboration, “Measurement of underlying event characteristics using charged particles in pp collisions at  $\sqrt{s} = 900$  GeV and 7 TeV with the ATLAS detector ”, *Phys. Rev. D* **83** (2011) 112001, [arXiv:1012.0791](#).
- [7] ALICE Collaboration, “Underlying Event measurements in pp collisions at  $\sqrt{s} = 0.9$  and 7 TeV with the ALICE experiment at the LHC”, *JHEP* **7** (2012) 116, [arXiv:1112.2082](#).
- [8] CMS Collaboration, “Jet and underlying event properties as a function of particle multiplicity in proton-proton collisions at  $\sqrt{s} = 7$  TeV ”, *Eur. Phys. J. C* **73** (2013) 2674, [arXiv:1310.4554](#).
- [9] I. Dremin and V. Nechitailo, “Proton periphery activated by multiparticle dynamics ”, *Nucl. Phys. A* **916** (2013) 241, [arXiv:1306.5384](#).
- [10] TOTEM Collaboration, “ Luminosity-independent measurements of total, elastic and inelastic cross-sections at  $\sqrt{s} = 7$  TeV”, *Europhys. Lett.* **101** (2013) 21004.

- [11] TOTEM Collaboration, “Measurement of proton-proton inelastic scattering cross-section at  $\sqrt{s} = 7$  TeV”, *Europhys. Lett.* **101** (2013) 21003.
- [12] I. Dremin, “Torus or black disk”, *JETP Lett.* **99** (2014) 243.
- [13] L. Frankfurt, M. Strikman, and C. Weiss, “Dijet production as a centrality trigger for p-p collisions at CERN LHC”, *Phys. Rev. D* **69** (2004) 114010, [arXiv:0311231](#).
- [14] CMS Collaboration, “Charged particle multiplicities in pp interactions at  $\sqrt{s} = 0.9, 2.36$  and 7 TeV”, *JHEP* **01** (2011) 079.
- [15] M. Strikman, “Comments on the observation of high multiplicity events at the LHC”, *Phys. Rev. D* **84** (2011) 011501.
- [16] CMS Collaboration, “Measurement of the inelastic proton-proton cross section at  $\sqrt{s} = 7$  TeV”, *Phys. Lett. B* **722** (2013) 5.
- [17] H. J. Drescher and M. Strikman, “How to probe high gluon densities in pp collisions at the Large Hadron Collider”, *Phys. Rev. Lett.* **100** (2008) 152002.